Performance of PM-Assisted Synchronous Reluctance Machine Under Rotor Eccentricity

Bishal Silwal[1, *], Mohamed N. Ibrahim[1, 2], Peter Sergeant[1,3]
[1]Department of Electrical Energy, Metals, Mechanical Constructions and Systems, Ghent University, Ghent 9000, Belgium
[2]Electrical Engineering Department, Kafrelshiekh University, Kafr el-Sheikh 33511, Egypt
[3]Flanders Make, the Strategic Research Center for the Manufacturing Industry, B-8500 Kortrijk, Belgium
e-mail*:bishal.silwal@ugent.be

***Abstract*— This paper deals with the study of a permanent magnet assisted synchronous reluctance machine (PMaSynRM) under static and dynamic rotor eccentricity. A 5.5 kW machine is used as the test machine, and the study is performed by using the finite element method. The influence of rotor eccentricity on several performance indicators of the PMaSynRM, such as, torque and losses is investigated.**

Keywords*— *eccentricity, finite element method, loss, permanent magnet assisted synchronous reluctance machine, torque

I. Introduction

For radial-flux machines, a concentric rotor may always not be a true case for various reasons, for instance, manufacturing defects or bearing failure, etc. Such defects causes rotor eccentricity. In some cases, the rotor might be shifted from the geometrical centerline of the stator but rotates in its own axis, which is called static eccentricity. When the shifted rotor rotates around the geometrical centerline of the stator with a certain frequency, the rotor is said to be under dynamic eccentricity (see Figure 1). Mixed eccentricity is the case when the rotor undergoes both static and dynamic eccentricities at the same time. The non-uniform air gap caused by rotor eccentricity creates an asymmetrical flux-density distribution around the air gap, which produces forces. The eccentricity force and the unbalanced magnetic pull (UMP) caused by it have been rigorously studied in the literature, in particular for induction machines [1-5]. Other machine types, for instance, permanent magnet (PM) machines, synchronous generators, switched reluctance (SR) machines, synchronous reluctance (SynRM) machines have also been adequately studied [6-14].

Besides the forces, it is also necessary to know how the machine under eccentricity performs in terms of several performance indicators, for example torque, losses, power factor, etc. The additional losses due to eccentricity in a cage induction machine is studied in [15]. Recently, [16, 17] investigated the influence of rotor eccentricity on the torque and its harmonics of a cage induction machine. Results showed an increased average torque and an influence on the harmonic components in the vicinity of the slot harmonics. Other factors like air gap flux-density, flux linkage, back-emf, torque, torque harmonics and losses of PMs have been studied in [18, 19]. The damper bar currents of a large hydro-generator have been studied both analytically and numerically in [20] and the performance of a SR machine has been predicted in [21]. However, very few literature regarding the performance of permanent magnet assisted synchronous reluctance machines (PMaSynRMs) during rotor eccentricity were found.

Synchronous reluctance machines have been gaining an immense popularity due to their high efficiency, low cost and robust structure. In addition, the torque density is much better than that of induction machines. However, the power factor of SynRMs is rather poor. In order to enhance the torque density and power factor of SynRMs, permanent magnets are inserted in the rotor flux-barriers, resulting in the well-known permanent magnet-assisted synchronous reluctance machines (PMaSynRM) [22, 23]. In this paper, the performance of an eccentric PMaSynRM is compared with that of a healthy case. Both static and dynamic eccentricity have been considered. Finite element method (FEM) was used for this purpose.

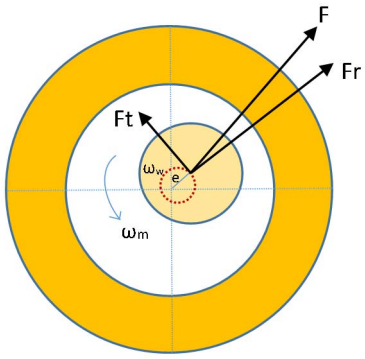

Fig. 1. Schematic representation of a radial-flux machine under eccentricity and the eccentricity forces.

II. Machine Model

A. Test Machine

A three-phase, four pole, 5.5 kW permanent magnet assisted synchronous reluctance machine is used in this study, the cross-sectional geometry of the is shown in Figure 2. The rotor has three flux barriers per pole and ferrite permanent magnets are inserted in the center of the flux barriers (see Figure 2). Ferrite magnets are preferred over rare earth magnets (e.g. NdFeB) because of thier low cost, the availability in the market. In addition, they can withstand high temperatures [23]. The geometrical parameters of the machine is give in Table I.

Identify applicable funding agency here. If none, delete this text box.

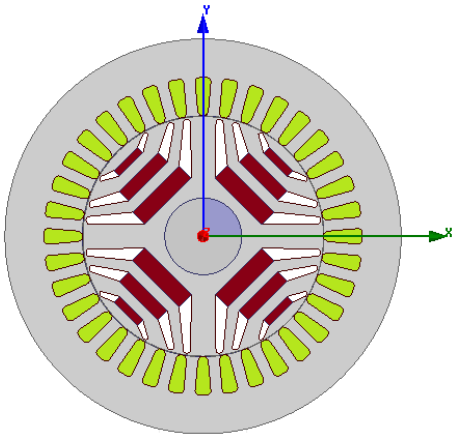

Fig. 2. Cross-sectional geometry of the permanent magnet assisted synchronous reluctance machine used in the study (PMaSynRM). Ferrite magnets are inserted in the center of the flux-barriers.

TABLE I. MACHINE PARAMETERS

Parameter	Value
Number of poles	4
Number of stator slots	36
Number of phases	3
Number of rotor flux barriers per pole	3
Stator outer/inner diameter	180/110 [mm]
Rotor outer/inner diameter	109.3/35 [mm]
Active axial length	140 [mm]
Rated power	5.5 kW
Rated voltage	380 [V]
Rated current	12.23 [A]
Rated speed	3000 [rpm]

B. FEM and Eccentricity

The machine used in the study is modelled in MAXWELL ANSYS software. A two-dimensional time-stepping method has been used in this study to compute the magnetic field solution across the cross-section of the machine. The time-stepping method is based on the magnetic vector potential formulation. The Maxwell field equations in the quasi-static state together with the constitutive material equations lead to the following equation to be solved in the cross-sectional geometry of the machine:

$$\nabla\times(\upsilon\nabla\times A)=-\sigma\left(\frac{\partial A}{\partial t}-\nabla\phi\right) \quad (1)$$

where, υ is the magnetic reluctivity and σ is the conductivity of the material, $\boldsymbol{A}$ is the magnetic vector potential and ϕ is the reduced electric scalar potential.

The stator windings are fed with three phase sinusoidal currents to emulate the current controlled inverter that supplies the machine. The rotor was rotated at its rated mechanical speed. The movement is done by moving band technique. To model the static eccentricity, the stator is shifted along the negative x-axis (see Figure 2) by a distance equal to the eccentricity radius such that the shortest air gap appears along the positive x-axis. To model the dynamic eccentricity, the rotor is moved along the positive x-axis by a distance equal to the eccentricity radius and then the rotor is rotated around the geometrical centerline of the stator. The eccentricity radius is equal to the eccentricity expressed as a percentage of the radial air gap length. For instance, if the eccentricity is set to 33%, the whirling radius equals 33% of radial air gap length.

The electromagnetic torque is calculated using the Maxwell stress tensor method, the expression for which is given as

$$T_e=\frac{l}{\mu_0}\int_0^{2\pi} r^2 B_r B_\theta \mathrm{d}\theta \quad (2)$$

where, l is the axial length of the machine, μ_0 is the permeability of free space, r is the radius of the integration, B_r and B_θ are the radial and tangential component of the magnetic flux density.

C. Loss Modeling

The materials used for the stator and rotor core construction are M270-50A and M330-50Am respectively. The stator windings constitute of copper wires. The copper loss in the stator windings are calculated from the current density J as

$$p_{cu}=\int_\Omega \frac{J^2}{\sigma} d\Omega \quad (3)$$

where, σ is the electrical conductivity of the material.

The core loss is divided into hysteresis loss, classical eddy current loss and excess loss and is calculated based on the Steinmetz equation [24] as

$$p_{core}=K_h B_{\max}^2 f+K_c(B_{\max}f)^2+K_e(B_{\max}f)^{1.5} \quad (4)$$

where, B_{max} is the maximum amplitude of the flux density, f is the frequency and K_h, K_c, K_e are the hysteresis coefficient, classical eddy coefficient and excess loss coefficient, respectively, which are all material dependent parameters.

III. INFLUENCE OF ECCENTRICITY

The goal of this paper is to present the influence of static and dynamic eccentricity on different performance indicators of the machine such as the magnetic flux density, torque, losses and efficiency. The non-uniform air gap during eccentricity causes the magnetic flux to be higher in the direction of shortest air gap. This is evident from Fig. 3 that shows the comparison between the flux density distribution in the cross-section of the machine in healthy case and the case with 55% dynamic eccentricity.

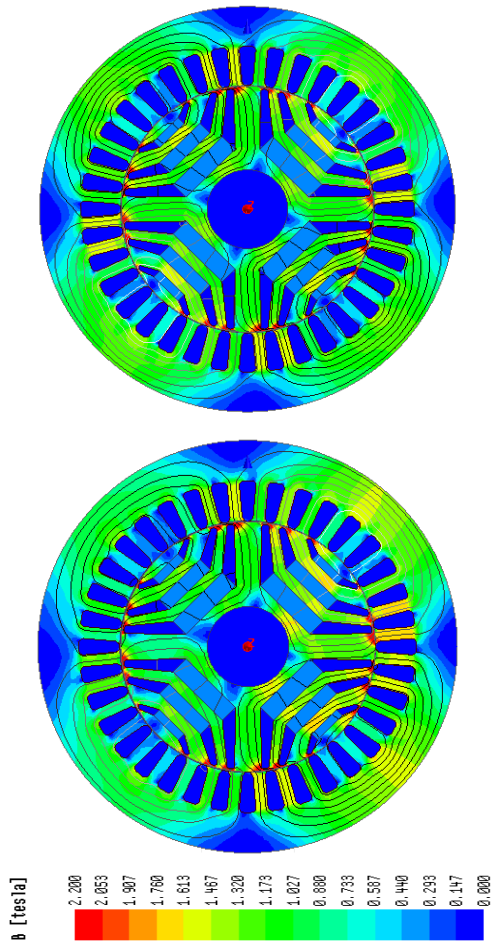

Fig. 3. Flux density distribution in the machine cross-section, in healthy condition (top) and with 55% dynamic eccentricity (bottom). The flux can be seen to be concentrated along the shortest air gap (right side in the figure) in the eccentric machine.

The asymmetrical flux-density distribution creates unbalanced force acting on the rotor. This force is mainly directed towards the shortest air gap. When the rotor is under static eccentricity, the position of the shortest air gap does not change. Therefore, the rotor experiences a radial pull in that direction. During dynamic eccentricity, the non-uniformity of the air gap is time dependent, meaning that the position of the shortest air gap changes. For this reason, the force during dynamic eccentricity is circulating in nature. The trace of the force vector for 55% dynamic eccentricity can be seen in Fig. 4. The force in this case also has a tangential component. For this reason, the unbalanced magnetic pull experienced by the rotor is more severe in case of static eccentricity than the dynamic eccentricity. The magnitude of the force exerted on the rotor in case of 55% static and dynamic eccentricity is plotted against time in Fig. 5. It is clear that force is slightly higher in the case of static eccentricity. The forces are calculated by integrating the Maxwell stress tensor in the air gap.

Fig. 6. shows the average output torque of the machine as a function of the current angle. Three cases, healthy, 33% static eccentricity and 33% dynamic eccentricity, have been considered. The simulations are performed at rated speed and rated current. It is evident from the figure that the optimal current angle at which the maximum torque is obtained remains the same. Nevertheless, there might be slight difference in the value of torque.

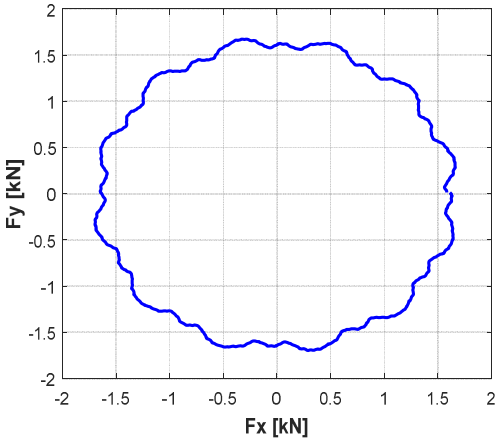

Fig. 4. The trace of the force vector when the rotor is under 55% dynamic eccentricity.

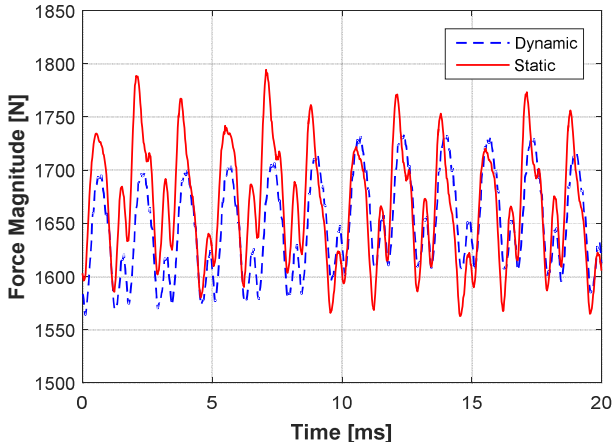

Fig. 5. Force exerted on the rotor when the rotor is under 55% eccentricity, both static and dynamic.

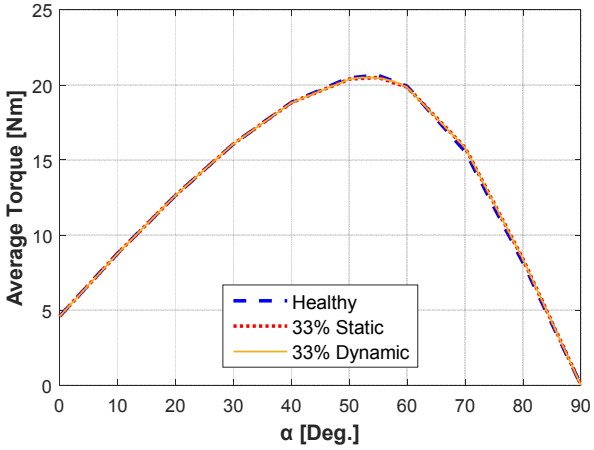

Fig. 6. Average output torque as a function of the current angle at rated condition

Although the difference in the average output torque between the eccentric and healthy cases is minimal, the difference in the torque ripple is rather significant. Fig. 7. shows the torque ripple as a function of the current angle for the aforementioned three cases. It is clear that the eccentricity affects the torque ripple, with high ripple in case of dynamic eccentricity. The time variation of the torque is shown in Fig. 8 at a current angle of 60°. The effect of eccentricity on the average torque is not significant. For instance, the difference between the torque of the healthy machine and the same machine under 33% dynamic eccentricity is around 0.3%, which can be neglected.

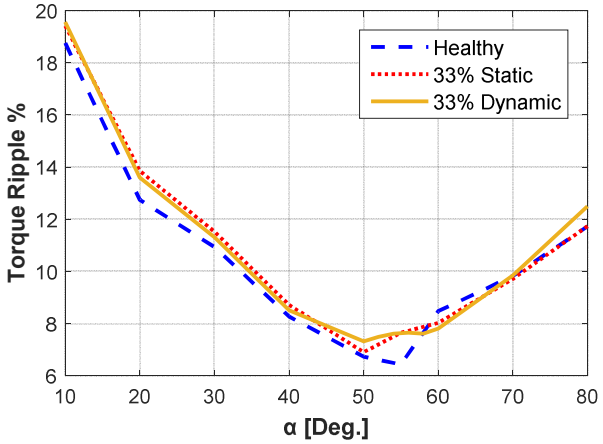

Fig. 7. Torque ripple as a function of the current angle at rated conditions

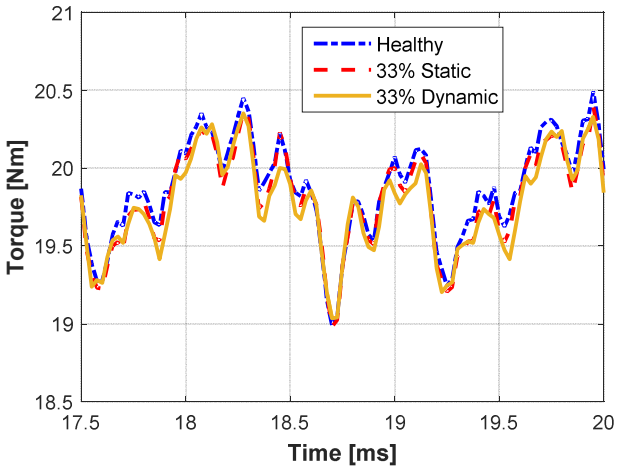

Fig. 8. Time variation of the torque at rated speed

Next, the influence of the eccentricity on the losses is studied. Fig. 9 and 10 show the core loss of the machine when the machine is under static eccentricity and dynamic eccentricity respectively. It can be well understood from the waveforms that the eccentricity has a significant effect in the core losses. In case of static eccentricity the difference in the core loss between a healthy machine and the machine with 77% eccentricity is around 14.3 Watt, which represents an increase of about 18%. In the case of dynamic eccentricity, the core loss is seen to be increased by around 31% when the eccentricity is 77%. The total loss in the machine, calculated as the sum of the core loss and the resistive loss in the stator windings is shown as a function of eccentricity in Fig. 11. Since the machine is fed through a pure sinusoidal current supply and the current density in the windings is uniformly distributed, the resistive loss does not change. The results shown in Fig. 9 to Fig. 11. are obtained for the current angle of 60°.

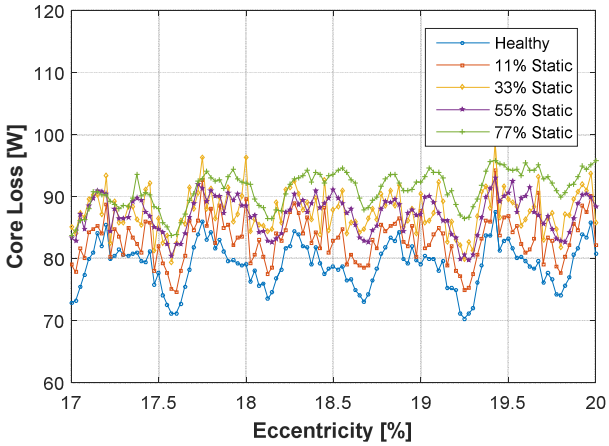

Fig. 9. Core loss in the machine with static eccentricity shown as a function of time.

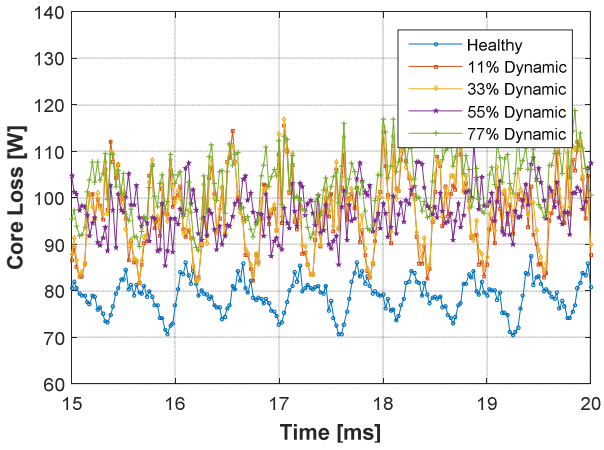

Fig. 10. Core loss in the machine with dynamic eccentricity shown as a function of time.

IV. Conclusion

The influence of static and dynamic rotor eccentricity on the force acting on the rotor torque and loss of a pm-assisted synchronous reluctance machine has been studied. Ansys Maxwell tool was used for the study. Results showed that the average torque of the machine is not significantly affected by eccentricity, however the torque ripple is seen to be higher in case of dynamic eccentricity. The current angle of the maximum output torque also remains unchanged. Nonetheless, the core loss of the machine appears to be much affected by eccentricity

and the performance is worse in the case of dynamic eccentricity. Therefore, eccentricity lowers the efficiency of the machine.

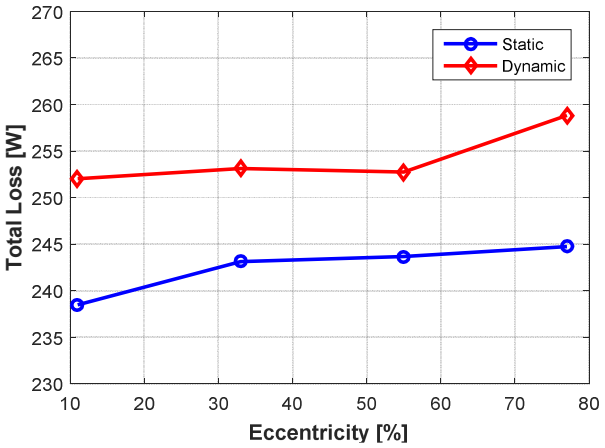

Fig. 11. Total loss in the machine as a function of eccentricity

REFERENCES

[1] A. Arkkio, M. Antila, K. Pokki, A. Simon, and E. Lantto, "Electromagnetic force on a whirling cage rotor," in IEE Proceedings - Electrical Power Application, vol. 147, no. 5, pp. 353–360, Sep. 2000.

[2] A. C. Smith and D. G. Dorrell, "Calculation and measurement of unbalanced magnetic pull in cage induction motors with eccentric rotors. I. Analytical model," in IEE Proceedings - Electrical Power Application, vol. 143, no. 3, pp. 193–201, May 1996.

[3] D. G. Dorrell and A. C. Smith, "Calculation and measurement of unbalanced magnetic pull in cage induction motors with eccentric rotors. II. Experimental investigation," in IEE Proceedings - Electrical Power Application, vol. 143, no. 3, pp. 202–210, May 1996.

[4] A. Arkkio, "Unbalanced magnetic pull in cage induction motors - dynamic and static eccentricity" in Proceedings of International Conference on Electrical Machines (ICEM), Spain, Sept. 1996, pp. 192–197.

[5] A. Tenhunen, "Electromagnetic forces acting between the stator and eccentric cage rotor", PhD Thesis, Helsinki University of Technology, Finland, 2003.

[6] M. Michon, R. Holehouse, K. Atallah, and J. Wang, "Unbalanced magnetic pull in permanent magnet machines," in Proceedings of 7th IET International Conference on Power, Electrical Machines and Drives (PEMD), April 2014, pp. 1–6.

[7] D. Dorrell, M. Popescu, C. Cossar, and D. Ionel, "Unbalanced magnetic pull in fractional-slot brushless pm motors," in IEEE Industry Application Society Annual Meeting (IAS), 2008, Oct. 2008, pp. 1–8.

[8] K. T. Kim, K. S. Kim, S. M. Hwang, T. J. Kim, Y. H. Jung, "Comparison of magnetic forces for IPM and SPM motor with rotor eccentricity," in IEEE Transactions on Magnetics, vol. 37, no. 5, pp. 3448– 3451, 2001.

[9] L. Lundstrom, R. Gustavsson, J. o. Aidanpaa, N. Dahlback and M. Leijon, "Influence on the stability of generator rotors due to radial and tangential magnetic pull force," in IET Electric Power Applications, vol. 1, no. 1, pp. 1-8, January 2007.

[10] R. Perers, U. Lundin and M. Leijon, "Saturation effects on unbalanced magnetic pull in a hydroelectric generator with an eccentric rotor," in IEEE Transactions on Magnetics, vol. 43, no. 10, pp. 3884-3890, Oct. 2007.

[11] C. G. C. Neves, R. Carlson, N. Sadowski, J. P. A. Bastos, N. S. Soeiro and S. N. Y. Gerges, "Vibrational behavior of switched reluctance motors by simulation and experimental procedures," in IEEE Transactions on Magnetics, vol. 34, no. 5, pp. 3158-3161, Sep 1998.

[12] N. R. Garrigan, W. L. Soong, C. M. Stephens, A. Storace and T. A. Lipo, "Radial force characteristics of a switched reluctance machine," in Conference Record of the 1999 IEEE Industry Applications Conference. Thirty-Forth IAS Annual Meeting (Cat. No.99CH36370), Phoenix, AZ, 1999, pp. 2250-2258 vol.4.

[13] H. Mahmoud and N. Bianchi, "Eccentricity in synchronous reluctance motors-part I: Analytical and finite-element models," in IEEE Transactions on Energy Conversion, vol. 30, no. 2, pp. 745–753, June 2015.

[14] H. Mahmoud and N. Bianchi, "Eccentricity in synchronous reluctance motors-part II: Different rotor geometry and stator windings," in IEEE Transactions on Energy Conversion, vol. 30, no. 2, pp. 754–760, June 2015.

[15] A. Belahcen and A. Arkkio, "Computation of additional losses due to rotor eccentricity in electrical machines," in IET Electric Power Applications, vol. 4, no. 4, pp. 259-266, April 2010.

[16] B. Silwal, P. Rasilo, A. Belahcen, A. Arkkio, "Influence of the rotor eccentricity on the torque of a cage induction machine" Archives of Electrical Engineering, vol. 66, no. 2, pp. 383-396, June 2017.

[17] B. Silwal, P. Rasilo, A. Haavisto, A. Belahcen and A. Arkkio, "Measurement of torque harmonics of a cage induction machine under rotor eccentricity," 18th International Conference on Electrical Machines and Systems (ICEMS), Pattaya, 2015, pp. 98-102.

[18] Z. Q. Zhu, M. L. Mohd Jamil and L. J. Wu, "Electromagnetic performance of interior permanent magnet machines with eccentricity," Eighth International Conference and Exhibition on Ecological Vehicles and Renewable Energies (EVER), Monte Carlo, 2013, pp. 1-8.

[19] B. M. Ebrahimi and J. Faiz, "Diagnosis and performance analysis of threephase permanent magnet synchronous motors with static, dynamic and mixed eccentricity," in IET Electric Power Applications, vol. 4, no. 1, pp. 53-66, January 2010.

[20] S. Keller, M. t. Xuan, J. j. Simond and A. Schwery, "Large low-speed hydro-generators-unbalanced magnetic pulls and additional damper losses in eccentricity conditions," in IET Electric Power Applications, vol. 1, no. 5, pp. 657-664, Sept. 2007.

[21] S. R. A. Arani and B. Ganji, "Performance prediction of switched reluctance motor under eccentricity fault," in IEEE International Conference on Environment and Electrical Engineering and IEEE Industrial and Commercial Power Systems Europe (EEEIC / I&CPS Europe 2017), Milan, 2017, pp. 1-6.

[22] M. N. Ibrahim, P. Sergeant, and E. M. Rashad, "Synchronous reluctance motors performance based on different electrical steel grades," in IEEE Transactions on Magnetics, vol. 51, no. 11, Nov. 2015.

[23] M. N. Ibrahim, E. M. Rashad, and P. Sergeant "Performance comparison of conventional synchronous reluctance machine and PM-assisted type with combined star-delta winding," in Energies, vol. 10, no. 1500, pp 1-18, Sept. 2017.

[24] C. P. Steinmetz, "On the Law of Hysteresis," in Transactions of the American Institute of Electrical Engineers, vol. IX, no. 1, pp. 1-64, Jan. 1892.